

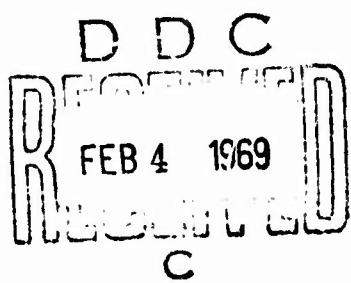
ARMY MATERIALS AND MECHANICS RESEARCH CENTER



036139 CW

AD

addl-5



Watertown, Massachusetts 02172

26

ACCESSION TO	
OPBT	WHITE SECTION
DDC	BUFF SECTION
UNANNOUNCED	
JUSTIFICATION	
SY	
DISTRIBUTION/AVAILABILITY CODES	
DIST.	AVAIL AND SPECIAL

The findings in this report are not to be construed as an official Department of the Army position, unless so designated by other authorized documents.

Mention of any trade names or manufacturers in this report shall not be construed as advertising nor as an official endorsement or approval of such products or companies by the United States Government.

DISPOSITION INSTRUCTIONS

Destroy this report when it is no longer needed.
Do not return it to the originator.

AMMRC TR 68-17

**TITANIUM CARBIDE CONTENT EFFECT ON
EROSION IN CERMET ROCKET NOZZLES**

Technical Report by

ANTHONY K. WONG and JAMES BROWN

October 1968

This document has been approved for public
release and sale; its distribution is unlimited.

**D/A Project 1C024401A328
AMCMS Code 5025.11.294
Metals Research for Army Materiel
Subtask 38089**

**METALS LABORATORY
ARMY MATERIALS AND MECHANICS RESEARCH CENTER
WATERTOWN, MASSACHUSETTS 02172**

ARMY MATERIALS AND MECHANICS RESEARCH CENTER

TITANIUM CARBIDE CONTENT EFFECT ON EROSION
IN CERMET ROCKET NOZZLES

ABSTRACT

Analyses were carried out on subscale cermet nozzles fired in the AMMRC solid propellant engine at a designated maximum chamber pressure of 1100 psi for nominal burning times of 15 seconds in order to determine mechanisms of erosion and the effect of the carbide constituent on erosion. The cermet class investigated consisted of an AISI Type 316 stainless steel matrix incorporating a hard phase of titanium carbide ranging in content from 20% to 55% by volume. The results of the study indicated that under the test conditions, increases in the titanium carbide constituents did increase the erosion resistance of the material. However, this was accomplished at the expense of thermal shock resistance. In addition, the mechanisms of erosion were determined to be thermal-chemical and mechanical in nature, manifested by both surface oxidation and thermal degradation of hardness and strength properties followed by the removal of discrete particles by the shearing action of the hot flowing gases. Erosion of the cermet nozzles was both asymmetrical and severe. Their erosion resistance was inferior to that of a lower density, commercial-grade graphite control nozzle tested under the same general conditions.

CONTENTS

	Page
ABSTRACT	
INTRODUCTION	1
TEST MATERIAL	
Composition and Fabrication	1
Properties	2
Microstructure	3
TEST PROCEDURES	
Nozzle Preparation	4
Firing Tests	4
Post Firing Analyses	8
RESULTS AND DISCUSSIONS	
Firing Tests	9
Post-Firing Analysis	12
CONCLUSIONS	18
LITERATURE CITED	19

INTRODUCTION

Cermets were originally developed by the Germans as a potential material for use in jet engine components. Their intention was to produce a material to bridge the properties gap between metals and ceramics. Further research in this country after World War II resulted in the development of many grades designed to combine the heat and oxidation resistance of ceramics with the thermal shock resistance and ductility of metals. Generally, cermets have been defined as a composite material composed of a hard phase incorporated within a softer metallic matrix or binder, and designated for applications involving high temperature environments. Consequently, cermets have received serious consideration for use in engine components such as rocket nozzles.

A rocket nozzle is subjected to high heat flux and highly erosive conditions from the hot combustion gases which must be exhausted through a properly contoured channel for the efficient development of thrust and control in the rocket engine. To function efficiently, a nozzle must remain intact throughout the duration of firing or must erode uniformly at a known, acceptable rate. Unexpected changes in the internal dimensions will deleteriously affect the burning characteristics of the propellant, thereby resulting in loss of thrust control. Erosion in the nozzle is manifested by the removal of material from the throat and other surfaces by chemical, mechanical, and thermal action. These phenomena are particularly serious in uncooled solid propellant rocket engines.

Because the heat transfer and erosion phenomena in rocket motors are highly complex in nature, actual firing tests on potential nozzle materials remain as one of the best analytical tools for evaluation purposes. The results of the investigation of the erosion resistance of a cermet composed of titanium carbide in a stainless steel matrix and the effects of carbide content are summarized in this report.

TEST MATERIAL

Composition and Fabrication

Cermet grades composed of titanium carbide, varying in nominal content between 20 and 55 volume percent in a matrix of AISI Type 316 stainless steel were specially formulated by the Sintercast Corporation of America for applications in which corrosion resistance and elevated temperature strength were prime requirements along with abrasion resistance.

Ten subscale rocket nozzles, each approximately 1.7 inches long with minor throat diameters of 0.3 inch, were purchased for this investigation. Figure 1 shows the general configuration and specified dimensions of the nozzles. Upon receipt of the nozzles, each was weighed and inspected for conformance with specification requirements. Despite the omission of a 45-degree external chamfer originally specified on the exit end of the nozzles, the lot was considered acceptable for this study. The cermet grades investigated contained 20, 30, 40, 50, and 55 percent titanium carbide. Two nozzles were fabricated from each grade.

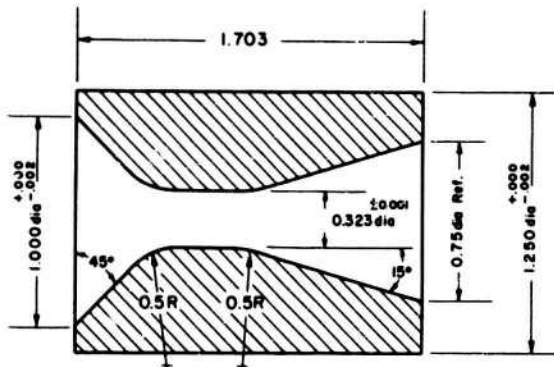


Figure 1. DIMENSIONS AND CONFIGURATION OF ROCKET NOZZLE

An infiltration technique,¹ which differs from the conventional powder metallurgical methods used in making cemented carbides for tools, was employed by the manufacturer in the processing of the cermet nozzles. The process involved the formation of a skeletal body of titanium carbide prepared by pressing the carbide powder at low pressures. A sintering operation was then used to impart coherence to the mass. Finally, the metallic matrix phase was introduced, in the liquid state, into the porous structure by the process of infiltration. An advantage claimed for this process is the formation of a product with improved toughness.

Properties

Measurements of the densities of the test materials revealed significant differences in values attributable to the varying compositions. A minimum average density determination of 6.18 g/cc was recorded for the cermet nozzle with the highest (55%) volume concentration of titanium carbide. This measured value was lower than expected and was more consistent with the density of that expected in a 60 percent grade. In comparison, the density of the heaviest cermet nozzle containing the lowest volume (20%) of the hard phase was determined to be 7.25 g/cc. The density of the intermediate grades varied between the aforementioned limits and decreased with increasing carbide content. Hardness, on the other hand, increased with increasing carbide content and ranged from 210 Brinell for the softest grade up to 455 for the hardest grade. These property variations and their associated carbide contents are indicated by the hardness and density measurements shown in Table I.

Table I. PROPERTIES OF CERMET ROCKET NOZZLES WITH AISI TYPE 316 STAINLESS STEEL MATRIX

Nozzle	TiC Content (vol. %)	Average Density (g/cc)	Brinell Hardness
19, 20	20	7.25	210
21, 22	30	7.03	271
23, 24	40	6.72	353
25, 26	50	6.42	412
27, 28	55	6.18	455

It also followed that the grades containing less titanium carbide in the structure were readily machinable while those containing larger volumes of carbide were more difficult to machine. Increases in the titanium carbide phase should increase the wear resistance of the cermet and render it more resistant to mechanical attack such as particle impingement.

X-ray spectroscopy was used to verify the composition of the matrix material. This rapid test indicated that the binder-phase composition was consistent with that of Type 316 stainless steel.

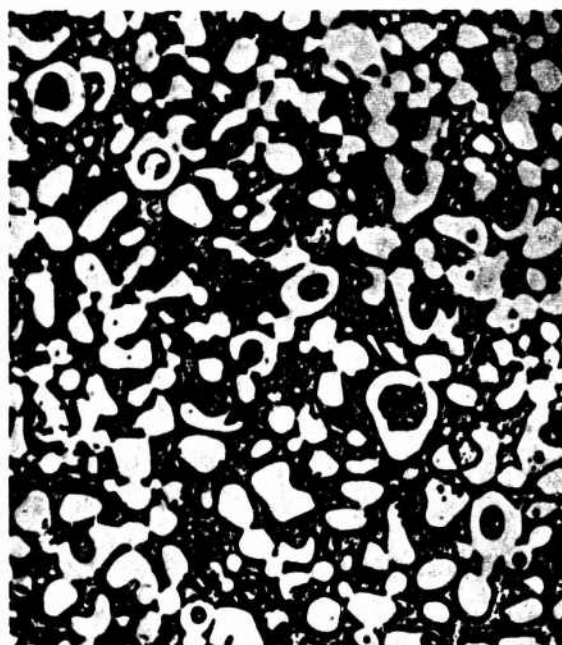
Microstructure

Microscopic examinations were made to inspect the microstructure of the cermets. An etchant composed of 20 cc HCl, 10 cc HNO₃, and 3 drops FeCl₃ was used to delineate the structure. The appearance of a polished and etched section of a typical area from the matrix-rich, 20% titanium carbide cermet is shown by the photomicrograph in Figure 2a. Under high magnification the presence of a lace-like network composed of small and large spherical-shaped particles was clearly evident. The smooth, gray particles were an integral part of the sintered titanium carbide skeleton and are shown in the photomicrograph to be encompassed in a matrix of austenitic stainless steel. Evidence of twinning was also observed in the infiltrated matrix structure. Some porosity, shown as black, irregular areas, was also noted in the surface. However, this condition was primarily attributed to pull-out of the hard phase during the metallurgical polishing process. In general, the microstructure appeared to be fairly sound and uniform throughout.

Subsequent microscopic examination of the 55% titanium carbide cermet revealed marked differences in the microstructure in comparison to the 20% carbide material. As shown by the photomicrograph in Figure 2b, the carbide phase quantitatively predominated in the structure in contrast to the more minor role exhibited in the earlier figure. Furthermore, the shape and appearance of the carbide phases provided direct contrast to each other. As shown in Figure 2b, the hard phase appeared to have been formed from smaller



a. 20 Percent TiC



b. 55 Percent TiC

Figure 2. ETCHED MICROSTRUCTURES OF TITANIUM CARBIDE-STAINLESS STEEL CERMETS. Mag. 1000X

particles which coalesced into a multitudinous number of round-edged shapes. Although the round edges should tend to promote thermal-shock-resisting characteristics, the high degree of coalescence of the particles tends to negate this advantage. Normally for improved mechanical and thermal shock resistance, a structure containing dispersed and isolated, fine spheroidal-shaped carbide grains is desirable. The hard phase was verified by Knoop hardness tests. In Figure 2b the gray shapes represent the carbide particles, while the more angular, bespeckled areas represent the infiltrated matrix phase; although some inhomogeneity was noted, the structure appeared to be relatively uniform throughout.

Within moderate limits, increases in the volume of titanium carbide in the body should be reflected by beneficial increases in strength and hardness. However, the advantage of these increases may be offset by the downgrading of other desirable properties such as toughness, thermal shock resistance, and ductility. In addition, fabrication variables necessitated by the change in the quantity of constituents may in themselves produce microstructural variations as evidenced by a comparison between the micrographs in Figures 2a and 2b. Consequently, compromises must be made between formulation and fabrication variables to maintain the proper balance of properties at an acceptable level.

Microstructures of the other grades of cermets were also examined and appeared to be intermediate to those shown in the preceding figures. Representative photomicrographs of the 30, 40, and 50 percent titanium carbide cermets are shown in Figure 3. With care, it was possible to distinguish the difference between the microstructures of the various specimens and to arrange them in ascending order based on carbide content.

TEST PROCEDURES

Nozzle Preparation

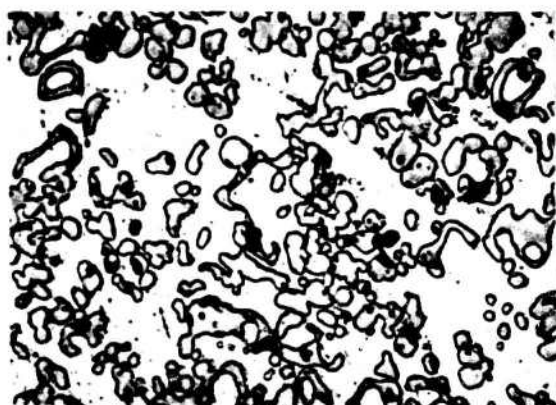
Using internal tri-point micrometers, the minor throat diameter of each nozzle was carefully measured and recorded. The nozzles selected for the firing tests were then cleaned with a solvent and oven-dried. Following this, the nozzles were individually slipped into thermal-insulating asbestos-reinforced plastic sleeves which were, in turn, pressed into heavy-walled steel nozzle mounts. A cross section of the nozzle holder assembly is shown in Figure 4. At the exit or exhaust end of the assembly, a steel retainer plate was bolted into place to provide firm longitudinal support for the nozzle. Although provisions were made in the holder for the incorporation of thermocouple glands, temperature measurements of the nozzle during the test were not made because of the temporary unavailability of instrumentation.

Firing Tests

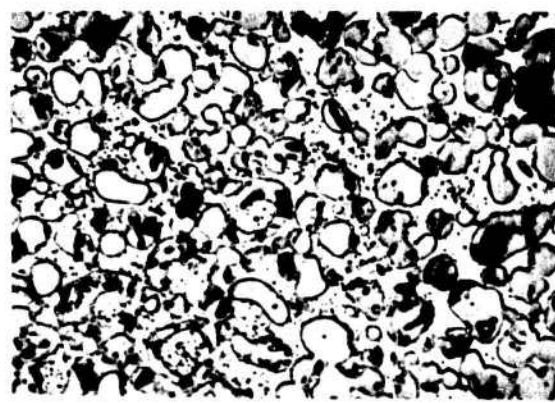
AMMRC's solid propellant, static test, variable parameter rocket engine was used in this study. The aforementioned nozzle holder assembly was threaded into the top plate of this unique vertical-firing engine. A simple configuration of this versatile static test engine is shown in Figure 5.



a. 30 Percent TiC



b. 40 Percent TiC



c. 50 Percent TiC

Figure 3. ETCHE MICROSTRUCTURES OF
INTERMEDIATE GRADES OF TITANIUM
CARBIDE-STAINLESS STEEL CERMETS. Mag. 1000X

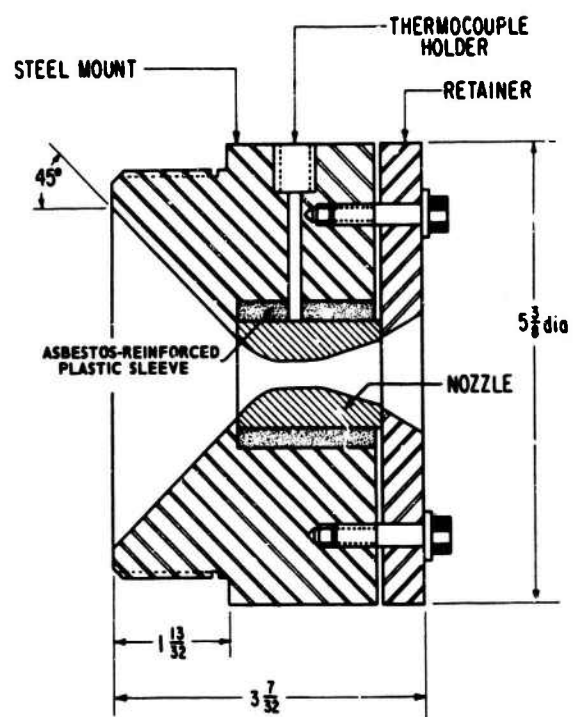


Figure 4. NOZZLE HOLDER ASSEMBLY
19-066-412/AMC-65

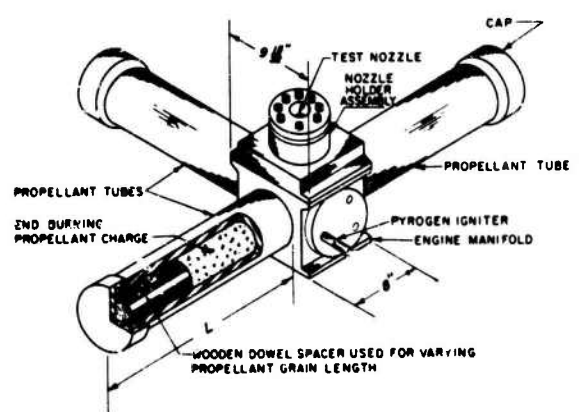


Figure 5. VARIABLE PARAMETER ROCKET ENGINE -
BASIC CONFIGURATION
19-066-425/ORD-60

Directly in line and below the test nozzle is a heavy-walled, central, cubic manifold which serves as a combustion chamber. Into this chamber, for this series of tests, were threaded two hollow steel propellant tubes each containing an end-burning solid-propellant grain. Neoprene O-rings were used throughout the assembly to prevent gas leakage. The third propellant tube shown in the illustration was fitted with a calibrated aluminum disk and served as a safety plenum chamber capable of absorbing minor overpressures generated during the combustion cycle.

The quantity of propellant tubes required for steady-state operation in this engine was determined by the following relationship:

$$N = \frac{A_b}{A_c} = \left[\frac{D_t}{D_c} \right]^2 \left[\frac{P_c^{(1-n)} g}{K C^* \rho_p} \right] \quad (1)$$

where:

N = number of charges

A_b = total propellant burning area

A_c = burning area of one charge

D_t = rocket nozzle throat diameter

D_c = propellant charge diameter

P_c = combustion chamber pressure

n = propellant burning rate exponent

g = gravitational constant

K = propellant burning rate coefficient

C^* = propellant characteristic velocity

ρ_p = propellant density

Furthermore, since the engine used end-burning charges, the length of the propellant charge was related to the total burning time as follows:

$$L = D_c P_c^n \cdot t_b \quad (2)$$

where:

L = length of charge and

t_b = propellant burning time.

The chamber pressure generated was a function of the nozzle throat diameter, the total propellant burning surface area (or number of charges), and the propellant properties.

The propellant used in this investigation was a nonaluminized Thiokol polymer, ammonium perchlorate formulation with a theoretical flame temperature of 4500 F. With two grains cut to predetermined lengths, securely potted into the propellant tubes, plans were made to carry out the tests at a maximum chamber pressure of 1100 psi for 15 seconds based on no erosion. However, erosion of the throat and the resultant increase in cross-sectional flow area will normally be manifested by a compensating decrease in chamber pressure along with an increase in the total burning time. The latter phenomenon is attributed to the fact that the propellant burning rate exponent normally decreases when the chamber pressure decreases.

Chamber pressure in this engine was measured through the use of a transducer-type load cell located in the base of the engine. Chamber pressure as a function of time data was indicated by an oscilloscope and recorded by a Polaroid Land camera. Ignition of the propellant was accomplished by means of a pyrotechnic igniter located in the side of the engine. Information on the operation of this nozzle test engine are discussed in greater detail in an earlier report.²

It is well recognized³ by rocket engine designers that tests of nozzles with various dimensions and configurations may well result in information that cannot be easily correlated. To minimize this problem, the nozzle used in this study was based on the design of the nozzle used in an investigation by Thiokol Chemical Corporation and Armour Research Foundation⁴ in their joint study of erosion mechanisms operating in uncooled rocket nozzles.

Two cermet nozzles, identified as 19 and 27, were selected for the initial firing tests. Upon completion of firing, four other cermet nozzles, 20, 21, 24, and 28, were also prepared and test fired in the rocket engine. Following each test, each jacketed nozzle was carefully removed from the holder using a wheel-pulling technique.

For test control purposes, another nozzle, machined from a bar of a high-quality commercial grade (National Carbon Company: CS) of extruded graphite with a bulk density of 1.68 g/cc, was prepared, preconditioned, and fired under conditions similar to that used in the test of the cermet nozzles. Although a variety of materials are being used as nozzle insert materials, graphite continues⁵ to be an attractive candidate material because of its exceptional combination of thermophysical characteristics. Contributing to its appeal is its high sublimation temperature (6700 F), low density, and increase in strength with increasing temperatures. Relative ease of fabrication and low cost are also important factors which make graphite a highly competitive nozzle material.

Post Firing Analyses

Following removal from the steel nozzle holder mount, the reinforced plastic jacket was carefully cut and removed from the circumference of each nozzle. Then each nozzle was gently cleaned with a soft brush to remove loose surface debris. Following this step, the nozzles were individually weighed on a balance scale and calculations made to determine weight loss. Except for erosion of the gas passages, the nozzles were intact. The appearance of the nozzles immediately after removal of the jackets is typified by the photograph in Figure 6. Visual examinations of the nozzles were also

made to determine extent of damage, while measurements were carried out to ascertain dimensional change. Shadowgraph enlargements were also applied as an aid in evaluating damage. However, extensive erosion in the exit and entrance cone regions of two of the nozzles minimized the effective application of this latter technique.

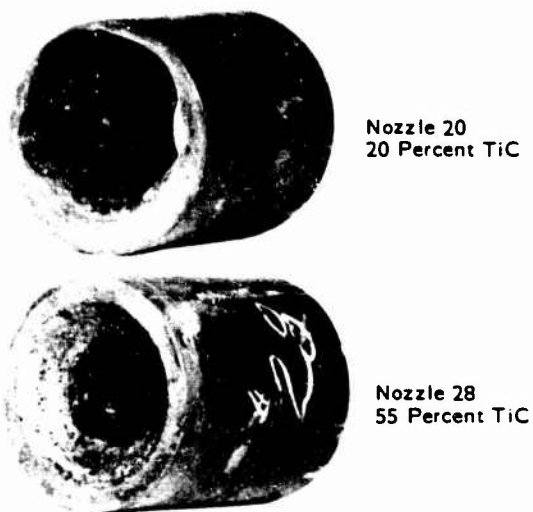


Figure 6. TWO NOZZLES AFTER REMOVAL FROM HOLDER

delineate the microstructure was composed of 20 cc HCl, 10 cc HNO₃, and 3 drops of FeCl₃. Following microscopic examinations at magnifications up to 1000, photomicrographs at 250X and 1000X were taken of representative areas. Some of these are included in this report. To supplement the metallographic examination, X-ray diffraction studies were also made of the structure in the region of the passageway surface-gas interface to determine the presence of reaction products and structural changes.

In addition, Brinell hardness measurements were made across the wall of the nozzles to determine the effects, if any, of the short exposure of the surface to the hot propellant gases. Several readings were made in selected areas and the results averaged.

RESULTS AND DISCUSSIONS

Firing Tests

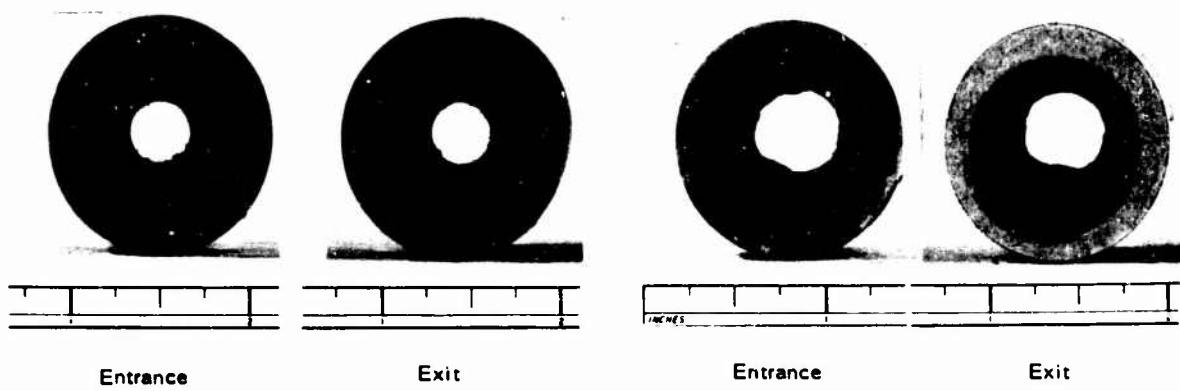
Nozzles 19, 20, 21, 24, 27, 28, and 66 were test fired in the solid propellant rocket engine shown in Figure 5. Since the data obtained from these tests were adequate, scheduled firings of nozzles 22, 23, 25, and 26 were judged to be unnecessary. The propellant grain in the engine was designed to produce a chamber pressure of 1100 psi for 15 seconds with the nozzle used in this investigation. These test conditions would, of course, be achieved only if the nozzle throat cross-sectional area remained constant. Enlargement or restrictions of this vital area would tend to decrease or increase the chamber pressure, respectively, since the propellant burning surface area in the engine remained essentially constant. Furthermore, the propellant burning constant would be affected by the chamber pressure and would tend to decrease with regression in gas pressure.

Nozzle 19, composed of 20% titanium carbide, was tested in the rocket engine at an outdoor ambient temperature of about 32 F. Under these test conditions, propellant gas condensation and nozzle blockage occurring during the initial stage of firing sufficiently reduced the throat cross-sectional area such that a chamber pressure in excess of 2000 psi was attained. Since this pressure was considerably greater than the planned chamber pressure of 1100 psi, the safety disk of the engine ruptured, spilling the exhaust gases out through a venting port.

Evaluation of the pressure-time traces obtained during the firings revealed that initial pressure rise was linear up to 1100 psi. This rise occurred in less than 1 second. Following the initial pressure rise, the pressure suddenly surged at a rapid rate, peaking at a point above 2000 psi in less than a second and diminishing only in response to the sudden diversion of gases through the pressure-activated, ruptured safety port.

However, the total exposure time of the nozzle to gas pressures in excess of 100 psi was less than 2 seconds. During this short time interval, the nozzle throat surface was eroded only to a minor degree, less than 6% increase in throat diameter. Furthermore, the nozzle orifice remained fairly symmetrical as shown by the exit and entrance end views presented on the left side in Figure 7. The rough-appearing throat region shown in silhouette was caused by a loosely adherent, black layer of material condensed from the propellant exhaust gases.

Immediately following the removal of the engine used to test nozzle 19, another preassembled engine was installed in place at the test site. Final electrical connections were made to the engine and nozzle 27, composed of 55% titanium carbide, was test fired. Upon ignition of the propellant, the chamber pressure rose in a satisfactory manner, attaining a magnitude of 1100 psi in about 1 second. The pressure-time trace also showed that the chamber pressure continued to rise to a maximum of 1175 psi. Analysis of the pressure-time trace indicated that erosion of the nozzle commenced 4 seconds after ignition as manifested by regression of chamber pressure at the rate of 170 psi



Nozzle 19, 20 Percent TiC

Nozzle 27, 55 Percent TiC

Figure 7. END VIEWS OF THE FIRST TWO NOZZLES TESTED

per second. Unfortunately, at the 7-second mark, a pressure surge occurred, momentarily increasing the chamber pressure to above 2000 psi. This transient condition, attributable to nozzle blockage, ruptured the safety disk of this engine thereby causing diminution of pressure which effectively terminated the test.

However, despite the short exposure time, the nozzle throat rapidly eroded under the destructive effect of the hot propellant gas. As shown in the righthand photographs of Figure 7, the throat surface eroded with a high degree of asymmetry and may be contrasted with that of the first nozzle shown in Figure 6. Despite the relative severity of erosion, visual inspection revealed that there were no thermal shock cracks present on the outer surface; the 55% titanium carbide cermet appeared to have withstood the combined effects of rapid heating and pressure rise.

In view of the limited nature of the data obtained in the first two firing tests, subsequent firings were made on related duplicate nozzles 20 and 28, containing 20% and 55% titanium carbide, respectively. As in the earlier tests, the engine was provided with sufficient propellant for producing a nominal chamber pressure of 1100 psi for 15 seconds. However, at this time the ambient test temperature was higher: 65 F.

No problems were encountered in preparing the engine for the test of nozzle 20, and the firing test was carried out in a routine manner. Upon ignition, the chamber pressure rose linearly, in 2-1/2 seconds, past the 1100 psi anticipated pressure up to a maximum of about 1300 psi. This overpressure may be attributable both to condensation of propellant burning by-products onto the nozzle throat wall and to unexpected changes in the propellant burning rate. The nozzle commenced to swiftly erode as evidenced by the rapid chamber-pressure regression at the initial rate of about 400 psi per second. The total burning time during the test was less than 15 seconds as is shown by the pressure-time trace in Figure 8.

In accordance with established procedures, another rocket engine assembly was set into the test stand and nozzle 28 was fired. Within 2 seconds after propellant ignition, a chamber pressure of 1600 psi was developed. However,

the nozzle exposure to this high pressure was only momentary as shown in Figure 9, a pressure-time trace obtained during the course of the test. As indicated by this trace, erosion of the nozzle throat in this constant burning surface area engine was manifested by a rapid drop in chamber pressure proceeding at a rate of about 900 psi per second, more than double that observed in the preceding test. Normally, this condition would imply that the erosion rate was greater in the 55% titanium carbide cermet nozzle than in the 20% titanium carbide cermet nozzle; however, subsequent post-firing examination of the nozzle indicated that this was not the case and that factors such as gas-flow characteristics must be taken into account. The remaining nozzles were fired in a similar manner.

Each of the nozzles was visually examined immediately after removal from the nozzle holder assembly. It was observed that the throat surfaces were eroded with varying degrees of asymmetry, as evidenced by the end views of selected nozzles shown in Figure 10. Furthermore, the asymmetry was especially pronounced at region of the exit cone in the nozzle with the lower carbide content. In addition, the total erosion occurring in nozzle 20 (20% TiC) appeared to surpass that of nozzle 28 (55% TiC) despite the fact that the propellant burning time at chamber pressures above 100 psi was about 20 seconds for the nozzle 28 in contrast to only 12 seconds for the nozzle 20. Although the operating conditions were severe enough to cause considerable erosion, no evidence of thermal cracking was observed on the outer surfaces.

However, the general appearance of the cermet nozzles compared unfavorably with that of the graphite control nozzle which was tested at an ambient temperature of 32 F under anticipated pressure and burning-time conditions similar to the earlier tests. As shown by the end view of graphite nozzle 66 (Figure 10), erosion of the graphite throat surface was minimal and relatively symmetrical in nature in direct contrast to the higher degree of erosion and asymmetry present in the cermet nozzles. Examination of the photograph also reveals the presence of an intermixed off-white and black layer which was condensed onto the graphite surface of the entrance cone during firing. However, its contribution to erosion was judged to be nil.

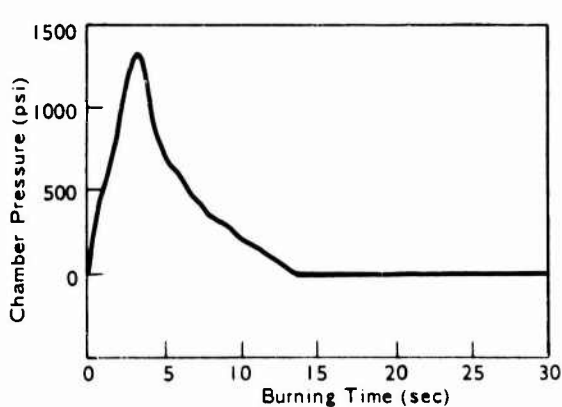


Figure 8. PRESSURE-TIME TRACE,
NOZZLE 20 - 20 PERCENT TiC

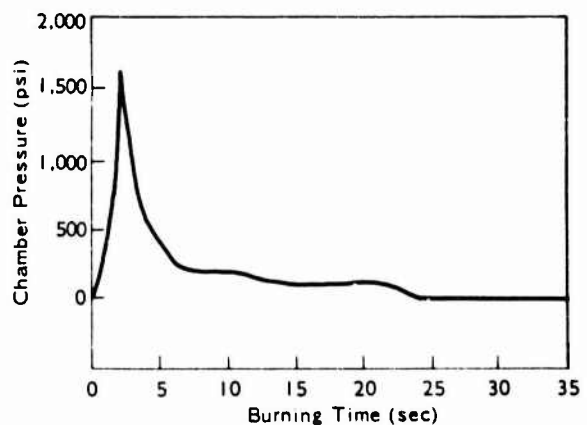


Figure 9. PRESSURE-TIME TRACE,
NOZZLE 28 - 55 PERCENT TiC

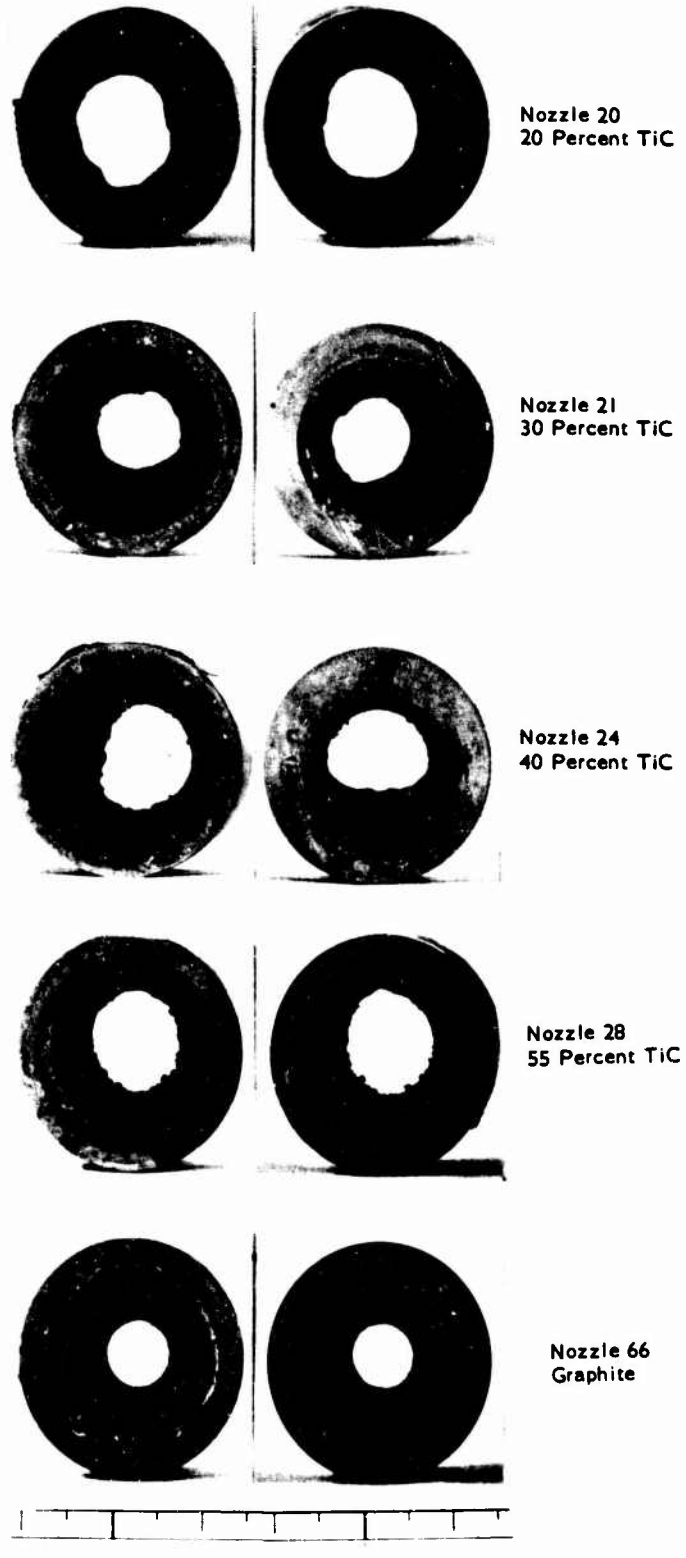


Figure 10. END VIEWS OF FIRED ROCKET NOZZLES

Data obtained during the test of the graphite nozzle are shown in the pressure-time trace in Figure 11. The curve indicated that the chamber pressure rose sharply in about 1 second following ignition. Thereupon, the pressure continued to increase, though at a slower rate, up to a maximum of about 1150 psi while maintaining the semblance of a plateau, signifying only small changes in the nozzle throat diameter. However, 16 seconds after ignition the pressure dropped rapidly, indicating burn-out of propellant. Based on the planned requirements, the performance of the graphite nozzle was judged to be highly satisfactory and consequently should provide an adequate base for comparison.

Post-Firing Analysis

Erosion, which occurred in all of the nozzles tested, was manifested by the removal of material from the inner wall surface, resulting in an increase in throat dimensions. However, erosion in nozzle 19 amounted to only 6 percent because of the short duration of exposure which was about only 1 second at chamber pressures above 100 psi. On the other hand, nozzle 27 suffered almost 50 percent increase in throat diameter despite its limited 8-second exposure to chamber pressures in excess of 100 psi. But these results cannot be reasonably compared because of the premature drop in chamber pressure caused by the release of gases through the ruptured safety disks during the tests. Therefore, the usefulness of the data obtained from the test of those two nozzles was extremely limited.

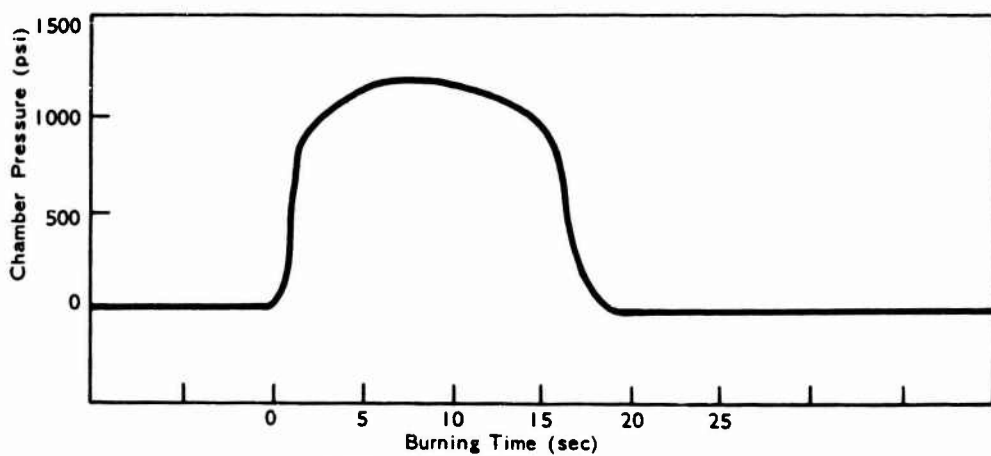


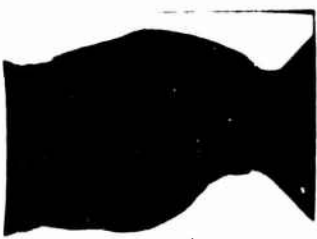
Figure 11. PRESSURE-TIME TRACE, Nozzle 66 - Graphite

Inasmuch as the firing tests on the remaining nozzles were carried out without mishap, a more meaningful comparison was made with the data obtained. Normally, measurements of changes in throat diameters are indicative of the degree of erosion encountered. However, as shown earlier in Figure 10, the removal of material from the throat and exit cone regions of the cermet nozzles was generally asymmetrical in nature. Consequently, simple diameter measurements would be meaningless in these cases. Since weight changes appeared to be more significant, this analytical procedure was undertaken. Analysis of data indicated that the matrix-rich nozzle, composed of only 20 percent titanium carbide, experienced a weight loss of 41 percent attributable to erosion.

Similar analysis of data from nozzle 28, composed of 55 percent titanium carbide, revealed that it experienced a weight loss of only 11 percent attributable to erosion. This was about one quarter of that encountered in nozzle 20. Weight loss in the remaining two nozzles with intermediate carbide content amounted to about 13 percent. General comparison of the weight-loss data indicated the increase in titanium carbide content in the cermet did indeed increase its erosion resistance capabilities. As expected, tests of the nozzles containing intermediate quantities of titanium carbide yielded increased erosion resistance in some proportion to the increased carbide content of the cermet.

To further examine the deleterious effects of the hot gases on the base material, the nozzle inserts were sectioned lengthwise. Cross sections of the walls and gas passages ranging from the entrance cone to exit cone of selected cermet nozzles and the graphite nozzle are shown in Figure 12. The erosive effects of the firing tests on the throat passageway are clearly evident.

Erosion in nozzle 28 was manifested by the methodical removal of material from the throat surfaces in a straightforward, though asymmetrical, progressive manner which in turn promoted a general, overall increase in both the length and diameter of the throat. In contrast to the relatively orderly erosion of material in the 55 percent TiC insert, Number 28, the erosion occurring in the 20 percent TiC insert, Number 20, was of a highly erratic nature manifested by extreme cavitation and guttering in different portions of the



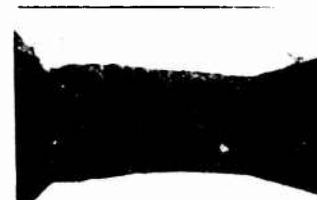
Nozzle 20
20 Percent TiC



Nozzle 21
30 Percent TiC



Nozzle 24
40 Percent TiC



Nozzle 28
55 Percent TiC



Nozzle 66
Graphite

→ Direction of Gas Flow

Figure 12. LONGITUDINAL CROSS-SECTION OF FIRED NOZZLE INSERTS

nozzle. This selective attack of surface material undoubtedly increased the turbulence of the hot flowing gases which then further increased the eccentric pattern of erosion.

Although the weight loss percent was similar in the two nozzle inserts with intermediate carbide content (30% and 40%), the mode of erosion was different. As shown in Figure 10, the failure of the lower carbide material eroded in a manner closely resembling that of the nozzle insert with 20 percent titanium carbide, manifested by guttering and cavitation effects. In contrast, the erosion in the 40 percent insert was relatively uniform in character, similar in shape to that which occurred in the 55 percent carbide insert, except slightly more severe.

For purposes of comparing erosion contours, Figure 12 also shows the longitudinal cross section of the graphite control nozzle. Cursory inspection of the section revealed that the graphite nozzle throat surface-gas interface and contour was essentially unaffected by the exposure to the hot propellant gases. However, closer inspection of the entrance cone, throat, and exit cone surfaces revealed the presence of a dark, off-white residue deposited by the exhaust gases. This loosely deposited layer did not materially impede the flow of gases.

Although the graphite control nozzle suffered only minimal damage during the firing sequence, it does not follow that all equivalent grade graphite nozzles fired under the same engine conditions would behave in the same fashion. The pretest condition of the nozzle played an important role in its erosion resistance. As stated earlier, the graphite control nozzle, as well as the cermet nozzles, was preconditioned by a dehydration process in an oven prior to the firing operation. The removal of moisture undoubtedly increased its erosion resistance. But if the nozzle was test fired, as it might under normal field

conditions, with absorbed moisture still entrained within its pores, the erosion rate would have been greatly enhanced. However, as shown by earlier studies⁶ at AMMRC pertaining to erosion mechanisms operating in graphite nozzles, the total enlargement of the throat of a good rocket-grade of graphite tested without preconditioning would, in all probability, be only one half of that which occurred in the carbide-rich cermet nozzle.

Quantitatively, the loss of surface material due to erosion in the graphite control nozzle amounted to 0.2 percent by weight as contrasted to 41 percent in nozzle 20 and 11 percent in nozzle 28. Considering factors such as test condition, density, and erosion pattern and resistance, graphite is superior to the titanium carbide-stainless steel cermets.

An extended examination was made of the nozzle sections to detect other damage to the structure attributable to the firing sequence. Examination of the cross-sectioned wall of nozzle 28 disclosed the presence of a semicontinuous crack extending in a partial loop along the length of the nozzle from the mid-region of the entrance cone to the mid-region of the exit cone. This condition is present in the photograph of the nozzle in Figure 12. Initiation and propagation of this crack is attributable to the inability of the high carbide material to adjust to the rapid temperature and pressure changes occurring during and after the firing cycle. As shown in the photograph, the terminal points of the crack were exposed to the hot gases and evidence of selective initial attack was present. Metallographic observations revealed that the propagation of the crack was primarily through the titanium carbide skeletal phase.

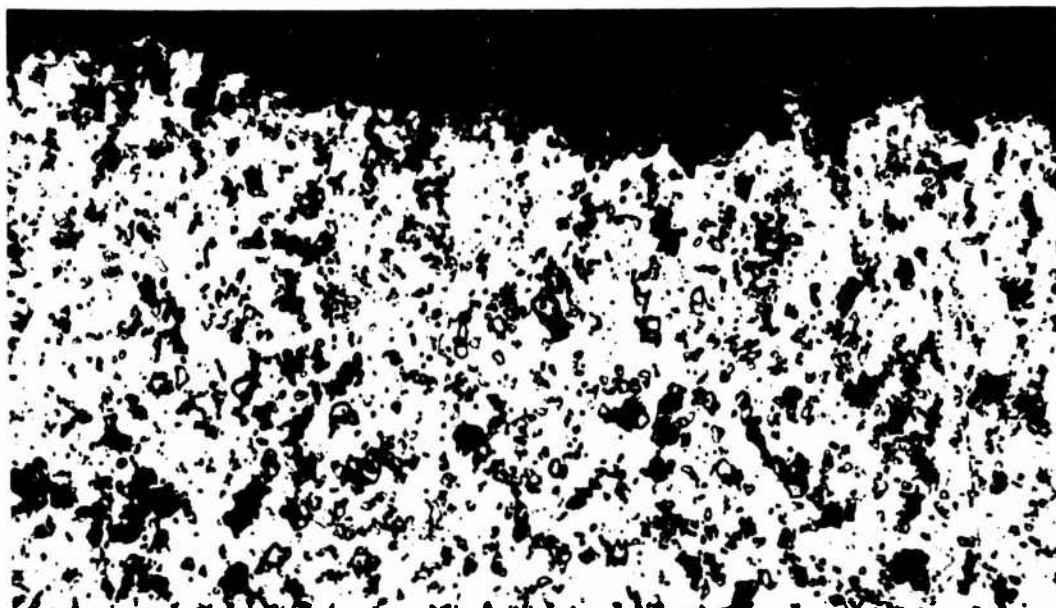
Similar examination of the sectional wall of the other nozzles did not reveal the presence of any cracks, thereby indicating that the matrix-rich cermet was sufficiently resistant to thermal shock. Therefore, it appears that while increasing the carbide content of the cermet to above 55 percent will increase the erosion resistance of the cermet, it will, in all probability, also decrease its thermal shock resistance to an unacceptable level. The formation of cracks during the firing sequence may produce regions susceptible to selective erosive attack. Even worse, catastrophic failure of the nozzle may occur, thereby causing complete failure of the rocket engine.

Post-test hardness studies were also carried out to determine the effect of the high gas temperatures, albeit for a short duration, on the cermet base material. It was discovered that the short exposure of the nozzle to the hot propellant gases was sufficient to soften the matrix material, particularly at the throat-gas interface of nozzle 20. The Brinell hardness at the throat surface of matrix-rich nozzle 20 decreased from a pre-firing average of 210 to an average of 155 after firing. The last figure closely approximates the hardness of annealed Type 316 stainless steel. This heat-affected zone extended from the throat surface-gas interface of the wall through to the outer surface of the nozzle with decreasing effect. At the outer surface of insert 20, the Brinell hardness was 200. The deterioration of hardness, along with shear strength, limits the usefulness of this grade of cermet for multiheating applications of the intensity encountered in the firing tests.

As expected, the carbide-rich cermet nozzle was slightly more resistant to the debilitating effects of heating. Post-firing measurements indicated a Brinell hardness drop from 445 to 415. Furthermore, this latter hardness value was found to be fairly uniform throughout the wall structure of nozzle 28. Indications are that this nozzle could be used in certain multiheating applications if erosion resistance was not a factor to be considered.

Metallographic examination of the surface-gas interface revealed an irregular profile caused by the removal of discrete particles from the surface by the moving gas stream. No visual evidence of incipient melting, plastic upsetting, or gross distortion of microstructures was observed, thereby indicating that the surface temperature remained somewhat below the 2500 F melting point⁷ of austenitic stainless steel. Figure 13 shows an unetched 250X magnification of a typical surface-gas interface region of nozzle 20. The microstructure below the eroded surface did not appear to be grossly affected by the heating phenomena. The formation and freeing of discrete particles appeared to be random in nature and did not preferentially occur in either the metal matrix or within the carbide-to-carbide network. However, penetrations and an increase in porosity was observed in the microstructure immediately adjacent to the eroded surface indicative of the debilitating effects of temperature, high velocity corrosive gases, and stresses. Softening of the metal matrix structure and chemical reactivity apparently lowered the shear resistance of the surface layer resulting in the progressive removal of the outermost material.

This latter condition was also observed in nozzle 28, though to a lesser degree. Figure 14 shows the microstructure of the throat surface-gas interface of the carbide-rich cermet. Metallograph observations at high magnifications of the surface layer revealed a paucity of the matrix substance

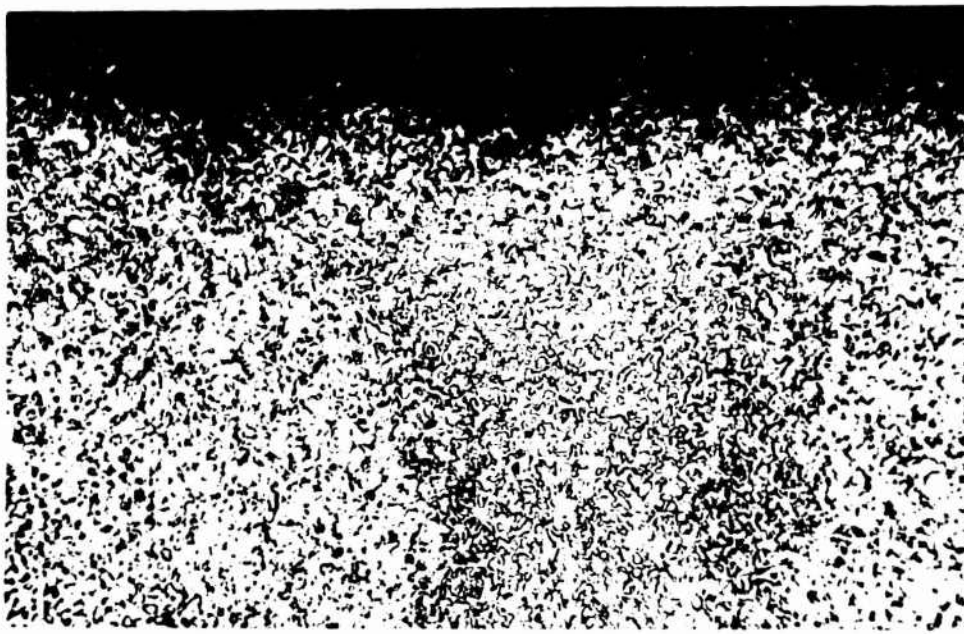


Unetched

20 Percent TiC

250X

Figure 13. MICROSTRUCTURE OF NOZZLE 20 THROAT SURFACE-GAS INTERFACE - AFTER FIRING



Unetched

55 Percent TiC

250X

Figure 14. MICROSTRUCTURE OF NOZZLE 28 THROAT SURFACE-GAS INTERFACE - AFTER FIRING

indicating initial sloughing out of the thermally softened metallic infiltrant followed by progressive disintegration of the surface of the weakened, unreinforced, hard-phase skeletal structure.

X-ray diffraction analyses were made to determine presence of reaction products within the throat surfaces of the nozzles. However, no measurable amounts were detected. Except for the loosely adherent deposits of propellant by-products, the base structure of the cermet remained essentially similar to the initial structure. Consequently, oxidation and corrosion was judged to have played a somewhat minor role in the erosion process. These results may be contrasted to the erosion⁸ in graphite nozzles wherein surface chemical reactions play an extremely important role.

As judged by available evidence, the process of erosion occurring in the cermet nozzle was primarily one of thermal degradation of the mechanical strength and hardness of the matrix of the material, partially accelerated by chemical reactivity, followed by the rapid removal of discrete particles from the surface under the shearing action of the high velocity propellant gases. Further, the quantity of erosion decreased with an increase in titanium carbide content. However, the rate of removal of the surface material from the cermet nozzles was excessive when compared to similar data obtained from the graphite control nozzle.

CONCLUSIONS

The results of this investigation revealed that the cermet grade containing 55 percent titanium carbide in Type 316 stainless steel matrix did indeed erode less than the grades composed of only 40, 30, and 20 percent, thereby implying that an increase in the carbide constituent will result in an increase in the erosion resistance. But a volumetric increase in the titanium carbide constituent to above 55 percent may degrade the thermal shock resistance of the cermet to an unacceptable level.

Furthermore, the erosion which occurred in the best cermet nozzle tested was more severe than that occurring in the graphite control nozzle. Thermal degradation of the mechanical strength, accelerated to a minor degree by chemical reactivity of the matrix material, followed by the removal of the weakened surface particles under the shear action of the high velocity propellant gases, appeared to be the primary mechanism of erosion.

In view of the serious degree of erosion encountered, this titanium carbide-stainless steel cermet is not recommended for use as an uncooled rocket nozzle, or as nozzle insert material subjected to environmental conditions similar to those used in this test.

LITERATURE CITED

1. SKOLNICK, L. P., and GOETZEL, C. *Titanium Carbide Products Produced by the Infiltration Technique*. Preprint No. 94g, American Society for Testing Materials, 1955.
2. LEVITT, A. P. *The Variable Parameter Rocket Engine - A New Tool for Rocket Nozzle Materials Evaluation*. Army Materials and Mechanics Research Center, WAL TR 766.1/2 (C), October 1960 (Confidential).
3. GOUSE, S. W. *Similitude in the Testing of Solid Propellant Rocket Nozzles*. Army Materials and Mechanics Research Center, AMRA TR 64-18, July 1964.
4. BASKIN, Y., and GREENING, T. *Study of the Mechanisms of Failure of Rocket Materials*. Armour Research Foundation, WADC Technical Report No. 58-152, August 1958.
5. WONG, A. K., and TARPINIAN, A. *Graphite as a Solid Propellant Rocket Nozzle Material*. Army Materials and Mechanics Research Center, AMRA MS 66-09, November 1966.
6. WONG, A. K., and LEVITT, A. P. *Graphite Nozzle Testing in a Solid Propellant Variable Parameter Rocket Engine*. Army Materials and Mechanics Research Center, AMRA TR 65-12, June 1965.
7. *Materials Selector, Materials in Design Engineering*. 1965, p. 22.
8. DELANEY, L. J., EAGLETON, L. C., and JONES, W. H. *A Semiquantitative Prediction of the Erosion of Graphite Nozzle Inserts*. American Institute of Aeronautics and Astronautics Journal, v. 2, no. 8, August 1964, p. 1428-1433.

UNCLASSIFIED

Security Classification

DOCUMENT CONTROL DATA - R&D

(Security classification of title, body of abstract and indexing annotation must be entered when the overall report is classified)

1. ORIGINATING ACTIVITY (Corporate author) Army Materials and Mechanics Research Center Watertown, Massachusetts 02172	2a. REPORT SECURITY CLASSIFICATION Unclassified
	2b. GROUP

3. REPORT TITLE**TITANIUM CARBIDE CONTENT EFFECT ON EROSION IN CERMET ROCKET NOZZLES****4. DESCRIPTIVE NOTES (Type of report and inclusive dates)****5. AUTHOR(S) (Last name, first name, initial)**Wong, Anthony K., and
Brown, James

6. REPORT DATE October 1968	7a. TOTAL NO. OF PAGES 19	7b. NO. OF REFS 8
8a. CONTRACT OR GRANT NO.	9a. ORIGINATOR'S REPORT NUMBER(S)	
b. PROJECT NO. D/A 1C024401A328	AMMRC TR 68-17	
cAMCMS Code 5025.11.294	9b. OTHER REPORT NO(S) (Any other numbers that may be assigned to this report)	
dSubtask 38089		

10. AVAILABILITY/LIMITATION NOTICES

This document has been approved for public release and sale; its distribution is unlimited.

11. SUPPLEMENTARY NOTES	12. SPONSORING MILITARY ACTIVITY U. S. Army Materiel Command Washington, D. C. 20315
-------------------------	--

13. ABSTRACT

Analyses were carried out on subscale cermet nozzles fired in the AMMRC solid propellant engine at a designated maximum chamber pressure of 1100 psi for nominal burning times of 15 seconds in order to determine mechanisms of erosion and the effect of the carbide constituent on erosion. The cermet class investigated consisted of an AISI Type 316 stainless steel matrix incorporating a hard phase of titanium carbide ranging in content from 20% to 55% by volume. The results of the study indicated that under the test conditions, increases in the titanium carbide constituents did increase the erosion resistance of the material. However, this was accomplished at the expense of thermal shock resistance. In addition, the mechanisms of erosion were determined to be thermal-chemical and mechanical in nature, manifested by both surface oxidation and thermal degradation of hardness and strength properties followed by the removal of discrete particles by the shearing action of the hot flowing gases. Erosion of the cermet nozzles was both asymmetrical and severe. Their erosion resistance was inferior to that of a lower density, commercial-grade graphite control nozzle tested under the same general conditions. (Authors)

DD FORM 1 JAN 64 1473

UNCLASSIFIED

Security Classification

UNCLASSIFIED

Security Classification

14. KEY WORDS	LINK A		LINK B		LINK C	
	ROLE	WT	ROLE	WT	ROLE	WT
Nozzles Rocket nozzles Solid propellants Cermets Titanium carbide Stainless steel Rockets Carbides Titanium Erosion						

INSTRUCTIONS

1. ORIGINATING ACTIVITY: Enter the name and address of the contractor, subcontractor, grantee, Department of Defense activity or other organization (corporate author) issuing the report.

2a. REPORT SECURITY CLASSIFICATION: Enter the overall security classification of the report. Indicate whether "Restricted Data" is included. Marking is to be in accordance with appropriate security regulations.

2b. GROUP: Automatic downgrading is specified in DoD Directive 5200.10 and Armed Forces Industrial Manual. Enter the group number. Also, when applicable, show that optional markings have been used for Group 3 and Group 4 as authorized.

3. REPORT TITLE: Enter the complete report title in all capital letters. Titles in all cases should be unclassified. If a meaningful title cannot be selected without classification, show title classification in all capitals in parentheses immediately following the title.

4. DESCRIPTIVE NOTES: If appropriate, enter the type of report, e.g., interim, progress, summary, annual, or final. Give the inclusive dates when a specific reporting period is covered.

5. AUTHOR(S): Enter the name(s) of author(s) as shown on or in the report. Enter last name, first name, middle initial. If military, show rank and branch of service. The name of the principal author is an absolute minimum requirement.

6. REPORT DATE: Enter the date of the report as day, month, year, or month, year. If more than one date appears on the report, use date of publication.

7a. TOTAL NUMBER OF PAGES: The total page count should follow normal pagination procedures, i.e., enter the number of pages containing information.

7b. NUMBER OF REFERENCES: Enter the total number of references cited in the report.

8a. CONTRACT OR GRANT NUMBER: If appropriate, enter the applicable number of the contract or grant under which the report was written.

8b, 8c, & 8d. PROJECT NUMBER: Enter the appropriate military department identification, such as project number, subproject number, system numbers, task number, etc.

9a. ORIGINATOR'S REPORT NUMBER(S): Enter the official report number by which the document will be identified and controlled by the originating activity. This number must be unique to this report.

9b. OTHER REPORT NUMBER(S): If the report has been assigned any other report numbers (either by the originator or by the sponsor), also enter this number(s).

10. AVAILABILITY/LIMITATION NOTICES: Enter any limitations on further dissemination of the report, other than those imposed by security classification, using standard statements such as:

- (1) "Qualified requesters may obtain copies of this report from DDC."
- (2) "Foreign announcement and dissemination of this report by DDC is not authorized."
- (3) "U. S. Government agencies may obtain copies of this report directly from DDC. Other qualified DDC users shall request through _____."
- (4) "U. S. military agencies may obtain copies of this report directly from DDC. Other qualified users shall request through _____."
- (5) "All distribution of this report is controlled. Qualified DDC users shall request through _____."

If the report has been furnished to the Office of Technical Services, Department of Commerce, for sale to the public, indicate this fact and enter the price, if known.

11. SUPPLEMENTARY NOTES: Use for additional explanatory notes.

12. SPONSORING MILITARY ACTIVITY: Enter the name of the departmental project office or laboratory sponsoring (paying for) the research and development. Include address.

13. ABSTRACT: Enter an abstract giving a brief and factual summary of the document indicative of the report, even though it may also appear elsewhere in the body of the technical report. If additional space is required, a continuation sheet shall be attached.

It is highly desirable that the abstract of classified reports be unclassified. Each paragraph of the abstract shall end with an indication of the military security classification of the information in the paragraph, represented as (TS), (S), (C), or (U)

There is no limitation on the length of the abstract. However, the suggested length is from 150 to 225 words.

14. KEY WORDS: Key words are technically meaningful terms or short phrases that characterize a report and may be used as index entries for cataloging the report. Key words must be selected so that no security classification is required. Identifiers, such as equipment model designation, trade name, military project code name, geographic location, may be used as key words but will be followed by an indication of technical context. The assignment of links, rules, and weights is optional.

UNCLASSIFIED

Security Classification